

Relationships between structure and high-throughput screening permeability of diverse drugs with artificial membranes: Application to prediction of Caco-2 cell permeability

Masaaki Fujikawa,^a Rieko Ano,^a Kazuya Nakao,^b Ryo Shimizu^b and Miki Akamatsu^{a,*}

^aGraduate School of Agriculture, Kyoto University, Kyoto 606-8502, Japan

^bTanabe Seiyaku Co., Ltd., Osaka 532-8505, Japan

Received 2 March 2005; accepted 28 April 2005

Available online 3 June 2005

Abstract—To evaluate the absorption of drugs with diverse structures across a membrane via the transcellular route, their permeability was measured using the parallel artificial membrane permeation assay (PAMPA). The permeability coefficients obtained by PAMPA were analyzed using a classical quantitative structure–activity relationship (QSAR) approach with simple physicochemical parameters and 3D-QSAR, VolSurf. We formulated correlation equations for diverse drugs similar to the equation obtained for peptide-related compounds in our previous study. The hydrogen-bonding ability of molecules, not only the hydrogen-accepting ability but also the hydrogen-donating ability, in addition to hydrophobicity at a particular pH, was significant in determining variations in PAMPA permeability coefficients. Based on this result, an *in silico* good prediction model for the passive transcellular permeability of diverse structural compounds was obtained. The artificial lipid-membrane permeability coefficients of the drugs, except salicylic acid, were well correlated with the Caco-2 permeability in a previous report suggesting the importance of absorption by the transcellular mechanism for these drugs.

© 2005 Elsevier Ltd. All rights reserved.

1. Introduction

The molecular properties for absorption, distribution, metabolism, and excretion (ADME) are crucial for drug design. Following oral administration, a drug must pass through intestinal cell membranes via passive diffusion, carrier-mediated uptake, or active transport processes before reaching the systemic circulation. The development of many potential drugs has been discontinued because of their poor absorption. Several screening paradigms that include absorption have been employed to enhance the probability of success through the drug development stage. Methods to assess absorption rely on *in situ*, *in vivo*, *in silico*, or *in vitro* models used alone or in combination.¹

As an *in vitro* method, Caco-2 cell monolayers are widely used to evaluate the intestinal absorption of compounds. Caco-2 cells express several kinds of transporter

proteins such as a peptide transporter² (PEPT1), monocarboxylic transporters³ (MCT), and an efflux system, P-glycoprotein⁴ (P-gp). Therefore, Caco-2 cell monolayers have the advantage that they incorporate both passive transport (transcellular or paracellular route) and active transporters. In contrast, the method using Caco-2 cells is rather labor-intensive and not easily applicable to high-throughput screening.

The parallel artificial membrane permeation assay (PAMPA) was proposed by Kansy et al. in 1998.⁵ PAMPA consists of hydrophobic filters coated with lecithin in an organic solvent solution. It is a rapid *in vitro* assay system that evaluates transcellular permeation and is applicable to high-throughput screening. PAMPA has been used for the prediction of oral absorption and blood–brain barrier penetration.^{6–14}

Previously, we measured the PAMPA permeability of peptide-related compounds such as protected peptides, cyclic peptides, and indole compounds as models of peptidomimetics.^{15,16} The classical quantitative structure–activity relationship (QSAR) procedure¹⁷ was then applied to the quantitative analysis between chemical structures and PAMPA permeability coefficients. The

Keywords: PAMPA; Artificial membrane permeability; Caco-2; Structure–property relationships.

* Corresponding author. Tel./fax: +81 75 753 6489; e-mail: akamatsu@kais.kyoto-u.ac.jp

classical QSAR, the so-called Hansch–Fujita approach, is a representative of QSAR methods and has been widely used in medicinal chemistry. The result of QSAR analysis showed that the hydrogen-accepting ability of molecules in addition to hydrophobicity at a particular pH was significant in determining the variations in PAMPA permeability coefficients. The compounds were then sorted according to their absorption pathway (passively transported compounds, actively transported compounds, and compounds excreted by efflux systems) in the plot of the Caco-2 cell and PAMPA permeability coefficients. Good correlation between Caco-2 cells and PAMPA permeability coefficients of passively transported compounds was obtained.

In this study, the PAMPA permeability of drugs with more diverse structures was measured and analyzed to investigate whether the permeability was determined by physicochemical properties similar to those of peptide-related compounds. In silico prediction of absorption was also discussed.

2. Results

2.1. Permeability with artificial membranes

Table 1 shows the permeability coefficient through the artificial membrane, $P_{\text{app-pampa}}$ values of 38 commercial drugs. We selected these compounds for the analyses because they are commonly used and have enough UV absorbance to measure the permeability using a UV plate reader. Their $\log P_{\text{oct}}$ and $\text{p}K_{\text{a}}$ values were in the range of -1.03 to 4.54 and 2.98 to 10.65 , respectively. In a previous study, classical QSAR analysis indicated the presence of the same absorption mechanism regardless of pH (6.3 and 7.3) in the acceptor compartment.¹⁶ Therefore, permeability at pH 7.3 was measured and used for the analyses in this study.

The $P_{\text{app-pampa}}$ values ranged from 0.19 (norfloxacin) to 38.53 (phenytoin) $\times 10^{-6}$ cm/s (8 drugs: $P_{\text{app-pampa}} < 1 \times 10^{-6}$ cm/s, 15 drugs: $1 \times 10^{-6} < P_{\text{app-pampa}} < 10 \times 10^{-6}$ cm/s, and 15 drugs: $P_{\text{app-pampa}} > 10 \times 10^{-6}$ cm/s). The relative standard deviation values of $P_{\text{app-pampa}}$ of all tested drugs were less than 50%, except nadolol.

2.2. Classical QSAR for the $\log P_{\text{app-pampa}}$

We quantitatively analyzed the PAMPA permeability, $\log P_{\text{app-pampa}}$, using the physicochemical parameters of the compounds, $\log P_{\text{oct}}$, where P_{oct} is the partition coefficient in the 1-octanol/water system, the absolute value of the difference between the $\text{p}K_{\text{a}}$ value of the compound and the experimental pH (7.3), $|\text{p}K_{\text{a}} - \text{pH}|$, and the surface area occupied by the hydrogen-bond acceptor and donor atoms of each modeled conformer, SA_{HA} and SA_{HD} . We obtained the following Eq. 1 for 35 commercial drugs. Imipramine, testosterone, and desipramine were excluded from the equation because they have high hydrophobicity and their measured $\log P_{\text{app-pampa}}$ values were smaller than those predicted from Eq. 1 (see Section 3).

$$\begin{aligned} \log P_{\text{app-pampa}} = & 0.40(\pm 0.09) \log P_{\text{oct}} \\ & - 0.29(\pm 0.08) |\text{p}K_{\text{a}} - \text{pH}| \\ & - 1.20(\pm 0.53) SA_{\text{HA}} \\ & - 0.78(\pm 0.56) SA_{\text{HD}} - 4.89(\pm 0.35), \\ n = 35, s = 0.27, r^2 = 0.84, q^2 = 0.79, \end{aligned} \quad (1)$$

where n is the number of compounds, s is the standard deviation, r is the correlation coefficient, q is the cross-validated (leave-one-out) correlation coefficient, and the figures in parentheses are the 95% confidence intervals. Eq. 1 indicates that membrane permeability increased with $\log P_{\text{oct}}$, and decreased as the $\text{p}K_{\text{a}}$ value was apart from experimental pH (pH 7.3). Furthermore, the larger surface area, occupied by the hydrogen-bond acceptor and donor atoms, was unfavorable for permeation through membranes.

As previously reported,¹⁶ classical QSAR Eq. 2 for $\log P_{\text{app-pampa}}$ at pH 7.3 of 22 peptide-related compounds was obtained using SA_{HA} .

$$\begin{aligned} \log P_{\text{app-pampa}} = & 0.56(\pm 0.15) \log P_{\text{oct}} \\ & - 0.27(\pm 0.12) |\text{p}K_{\text{a}} - \text{pH}| \\ & - 2.34(\pm 0.70) SA_{\text{HA}} - 5.14(\pm 0.36), \\ n = 22, s = 0.27, r^2 = 0.85, q^2 = 0.77. \end{aligned} \quad (2)$$

For 57 combined compounds, including 35 commercial drugs and 22 peptide-related compounds, the following Eq. 3 was formulated:

$$\begin{aligned} \log P_{\text{app-pampa}} = & 0.42(\pm 0.09) \log P_{\text{oct}} \\ & - 0.26(\pm 0.07) |\text{p}K_{\text{a}} - \text{pH}| \\ & - 1.11(\pm 0.47) SA_{\text{HA}} \\ & - 1.01(\pm 0.41) SA_{\text{HD}} - 4.93(\pm 0.30), \\ n = 57, s = 0.32, r^2 = 0.78, q^2 = 0.74. \end{aligned} \quad (3)$$

In Eqs. 1 and 3, the coefficients of the corresponding terms and the intercept were identical within 95% confidence intervals, indicating that the same physicochemical properties contributed to PAMPA permeability regardless of chemical structures. The $\log P_{\text{app-pampa}}$ values calculated by Eq. 3 are listed in Table 1. Figure 1 shows the correlation between the observed and calculated values. The development of Eq. 3 is shown in Table 2.

2.3. Effect of testosterone on permeability coefficients

The addition of cholesterol molecules to the lecithin bilayer is known to allow closer molecular packing and to reduce the mobility of the fatty acid chain of the lecithin.¹⁸ Since the presence of the high concentration of testosterone, which is a steroid like cholesterol, may change properties of the lecithin membrane and influence the permeability coefficient of compounds,¹⁹ the effect of testosterone on permeability coefficients was investigated. The permeability coefficient of the 500 μM pindolol, furosemide, propranolol, and verapamil was determined in the presence of 5, 50, and 500 μM testosterone. Dependence of $\log P_{\text{app-pampa}}$ of the four compounds on the testosterone concentration is shown in Figure 2. The permeability coefficient was approxi-

Table 1. Permeability coefficients of tested compounds and their QSAR parameters

No.	Compound	Group ^a	$P_{app-pampa}^b$ ($\times 10^{-6}$) (cm/s)	$\log P_{app-pampa}$		$\log P_{app-Caco-2}^d$	$\log P_{oct}$	$C \log P$	p <i>K</i> _a – pH	calcd p <i>K</i> _a – pH	PSA^e	SA_{HA}^f	SA_{HD}^g	MW	
				Measured	Calculated ^c										
Peptide-related compounds															
1	Boc-Trp	1	1.84	[0.99]	–5.74	–5.81	–5.67	2.65	2.80	3.60	3.30	0.995	0.557	0.438	304
2	Cbz-Trp	1	2.82	[0.95]	–5.55	–5.67	–5.80	3.20	3.25	3.60	3.32	1.076	0.637	0.439	338
3	Fmoc-Trp	1	12.75	[1.36]	–4.89	–4.96	–4.76	4.93	5.08	3.60	3.41	1.097	0.658	0.439	426
4	Trp-NH ₂	—	2.73	[0.27]	–5.56	–5.88	—	0.30	–0.15	0.20	0.88	0.982	0.320	0.661	203
5	Ac-Trp-NH ₂	1	1.92	[0.36]	–5.72	–5.71	–5.63	0.42	–0.19	0.00	0.00	0.907	0.419	0.488	245
6	Gly-Trp-NH ₂	—	0.42	[0.21]	–6.38	–6.56	—	–0.48	–1.76	0.00	0.00	1.363	0.530	0.832	260
7	Phe-Trp-NH ₂	—	5.98	[0.61]	–5.22	–5.76	—	1.38	1.01	0.00	0.00	1.345	0.513	0.833	350
8	Trp-Ala-Val-NH ₂	—	0.24	[0.05]	–6.62	–6.44	—	0.40	0.26	0.00	0.00	1.593	0.663	0.930	373
9	Ac-Trp-Val-NH ₂	3	0.66	[0.48]	–6.18	–6.02	–6.77	0.73	0.48	0.00	0.00	1.320	0.635	0.685	344
10	Ac-D-Trp-Val-NH ₂	3	0.73	[0.73]	–6.14	–5.91	–6.92	0.65	0.48	0.00	0.00	1.184	0.541	0.643	344
11	Ac-Tyr-Leu-NH ₂	—	0.29	[0.11]	–6.54	–6.05	—	0.32	0.35	0.00	0.00	1.183	0.527	0.657	335
12	Ac-Tyr-Phe-NH ₂	—	0.12	[0.10]	–6.92	–6.17	—	0.54	0.31	0.00	0.00	1.381	0.713	0.668	369
13	cyclo(-Trp-Gly)	1	0.97	[0.70]	–6.02	–5.92	–6.12	0.07	–0.32	0.00	0.00	0.961	0.509	0.452	243
14	cyclo(-Trp-Tyr)	—	0.68	[0.70]	–6.17	–5.74	—	1.11	1.47	0.00	0.00	1.201	0.621	0.580	349
15	cyclo(-Trp-Trp)	3	9.10	[1.99]	–5.04	–5.25	–5.92	2.04	2.13	0.00	0.00	1.119	0.533	0.586	372
16	Indole	1	31.91	[7.17]	–4.50	–4.26	–4.24	2.14	2.13	0.00	0.00	0.228	0.079	0.149	117
17	Tryptophol	1	19.11	[2.02]	–4.72	–4.80	–4.24	1.54	1.32	0.00	0.00	0.491	0.196	0.295	147
18	Tryptamine	—	5.42	[1.24]	–5.27	–5.68	—	1.35	1.42	2.90	3.27	0.551	0.124	0.427	160
19	Indole-3-acetamide	2	6.18	[0.56]	–5.21	–5.34	–4.23	0.75	0.44	0.00	0.00	0.693	0.280	0.414	174
20	Indole-3-carboxylic acid	2	0.79	[0.05]	–6.10	–5.63	–4.56	1.99	2.13	3.10	3.24	0.689	0.398	0.291	161
21	Indole-3-acetic acid	2	0.40	[0.02]	–6.40	–5.80	–4.85	1.41	1.40	3.00	2.81	0.641	0.362	0.279	175
22	Indole-3-propionic acid	2	2.10	[0.73]	–5.68	–5.57	–4.67	1.75	1.89	2.60	2.53	0.656	0.366	0.290	189
Drugs															
23	Acebutolol	1	0.36	[0.04]	–6.44	–5.83	–6.29	1.71	1.70	2.11	1.80	1.006	0.582	0.424	336
24	Acetaminophen	—	0.91	[0.27]	–6.04	–5.95	—	0.51	0.49	2.20	2.56	0.624	0.331	0.293	151
25	Alprenolol	1	11.50	[0.86]	–4.94	–4.83	–4.60	2.89	2.65	2.30	1.86	0.493	0.211	0.281	249
26	Antipyrine	—	2.87	[0.12]	–5.54	–5.14	—	0.23	0.20	0.00	0.00	0.279	0.279	0.000	188
27	Caffeine	1	3.92	[1.28]	–5.41	–5.73	–4.51	–0.07	–0.06	0.00	0.00	0.695	0.695	0.000	194
28	Chloramphenicol	—	3.89	[0.39]	–5.41	–5.72	—	1.14	1.28	0.00	0.00	1.181	0.790	0.391	323
29	Clonidine	1	10.41	[1.20]	–4.98	–5.01	–4.66	1.43	1.41	0.75	0.80	0.468	0.182	0.286	230
30	Corticosterone	1	16.81	[2.10]	–4.77	–4.95	–4.67	1.94	2.32	0.00	0.00	0.777	0.517	0.261	346
31	Coumarin	—	27.99	[3.09]	–4.55	–4.71	—	1.39	1.41	0.00	0.00	0.330	0.330	0.000	146
32	Dexamethasone	1	4.26	[0.36]	–5.37	–5.16	–4.91	2.01	1.75	0.00	0.00	1.007	0.587	0.420	392
33	Dilthiazem	—	19.21	[1.61]	–4.72	–4.64	—	2.80	3.65	0.76	1.64	0.783	0.628	0.000	415
34	Furosemide	—	0.34	[0.05]	–6.47	–6.65	—	2.03	1.87	3.96	4.26	1.443	0.868	0.570	331
35	Hydrochlorothiazide	1	0.20	[0.02]	–6.69	–6.59	–6.29	–0.07	–0.40	0.00	0.00	1.525	0.964	0.549	298
36	Hydrocortisone	1	3.53	[0.82]	–5.45	–5.27	–4.85	1.61	1.70	0.00	0.00	0.951	0.560	0.391	362
37	Ibuprofen	—	21.15	[7.85]	–4.67	–4.68	—	3.50	3.68	2.92	2.89	0.430	0.299	0.131	206
38	Imipramine ^h	—	19.36	[3.92]	–4.71	—	—	4.44	5.04	2.10	2.19	0.073	0.073	0.000	280
39	Ketoprofen	—	2.84	[0.14]	–5.55	–5.07	—	3.12	2.76	3.01	3.07	0.615	0.471	0.144	254
40	Labetalol	1	6.60	[0.56]	–5.18	–5.31	–5.03	3.09	2.50	2.10	1.90	1.085	0.416	0.669	328
41	Metoprolol	1	7.93	[3.91]	–5.10	–5.44	–4.63	1.88	1.35	2.45	1.87	0.622	0.341	0.281	267
42	Nadolol	1	0.71	[0.50]	–6.15	–6.26	–5.41	0.71	0.38	2.37	1.87	0.957	0.409	0.549	309

(continued on next page)

Table 1 (continued)

No.	Compound	Group ^a	$P_{\text{app-pampa}}^b$ ($\times 10^{-6}$) (cm/s)	$\log P_{\text{app-pampa}}$		$\log P_{\text{app-Caco-2}}^d$	$\log P_{\text{oct}}$	$C\log P$	$ \text{p}K_a - \text{pH} $	$ \text{calcd } \text{p}K_a - \text{pH} $	PSA^e	SA_{HA}^f	SA_{HD}^g	MW
				Measured	Calculated ^c									
43	Naproxen	—	5.01 [0.36]	−5.30	−4.95	—	3.34	2.82	3.29	2.46	0.532	0.401	0.130	230
44	Norfloxacin	—	0.19 [0.08]	−6.71	−6.78	—	−1.03	−0.99	2.08	1.34	0.808	0.560	0.248	319
45	Oxprenolol	—	14.64 [6.07]	−4.83	−5.31	—	2.10	2.09	2.30	1.87	0.624	0.362	0.262	265
46	Pindolol	1	4.91 [1.53]	−5.31	−5.48	−4.78	1.75	1.67	2.24	1.90	0.670	0.257	0.413	248
47	Practolol	—	1.06 [0.09]	−5.98	−6.06	—	0.79	0.75	2.10	1.86	0.858	0.435	0.423	266
48	Prednisolone	—	3.37 [0.41]	−5.47	−5.29	—	1.62	1.38	0.00	0.00	0.982	0.561	0.420	360
49	Propranolol	1	26.33 [4.02]	−4.58	−4.78	−4.66	2.98	2.75	2.30	1.84	0.483	0.209	0.274	258
50	Ranitidine	1	0.88 [0.10]	−6.05	−6.05	−6.31	0.27	0.63	0.88	1.10	1.095	0.699	0.222	314
51	Salicylic acid	2	1.21 [0.60]	−5.92	−5.88	−4.66	2.26	2.19	4.32	4.29	0.730	0.444	0.286	138
52	Testosterone ^h	—	11.20 [3.10]	−4.95	—	−4.60	3.32	3.22	0.00	0.00	0.447	0.307	0.140	288
53	Theophylline	—	4.84 [1.21]	−5.31	−5.75	—	−0.02	−0.06	0.00	0.00	0.746	0.611	0.135	180
54	Trimethoprim	—	3.14 [0.42]	−5.50	−5.85	—	0.91	0.88	0.00	0.00	1.219	0.658	0.561	290
55	Verapamil	—	23.02 [3.74]	−4.64	−4.48	—	3.79	4.47	1.36	1.68	0.717	0.717	0.000	455
56	Aminopyrine	1	17.29 [1.03]	−4.76	−4.80	−4.44	1.00	0.57	0.00	0.00	0.266	0.266	0.000	231
57	Desipramine ^h	1	16.98 [1.70]	−4.77	—	−4.61	4.54	4.47	3.35	3.10	0.185	0.048	0.137	266
58	Phenytoin	1	38.53 [10.32]	−4.41	−4.74	−4.57	2.26	2.08	0.00	0.00	0.708	0.441	0.267	252
59	Piroxicam	1	10.87 [1.76]	−4.96	−5.81	−4.45	1.98	1.89	2.23	2.80	1.045	0.798	0.241	351
60	Pirenzepine	1	0.89 [0.19]	−6.05	−5.91	−6.36	0.10	0.17	0.70 ⁱ	0.42	0.765	0.618	0.147	331

^a Compounds were classified into three groups according to their main transport mechanism. See text and Ref. 15 for the detail.^b The measurement was repeated at least four times. Values in parentheses are the standard deviation.^c Calculated from Eq. 3.^d Caco-2 permeability coefficients. From Ref. 21.^e van der Waals surface area ($\text{\AA}^2 \times 1/100$) occupied by polar atoms.^f van der Waals surface area ($\text{\AA}^2 \times 1/100$) occupied by hydrogen-bond acceptor atoms.^g van der Waals surface area ($\text{\AA}^2 \times 1/100$) occupied by hydrogen-bond donor atoms.^h These compounds were excluded from the analyses of PAMPA permeability.ⁱ Estimated from the $\text{p}K_a$ values of piperazine derivatives.

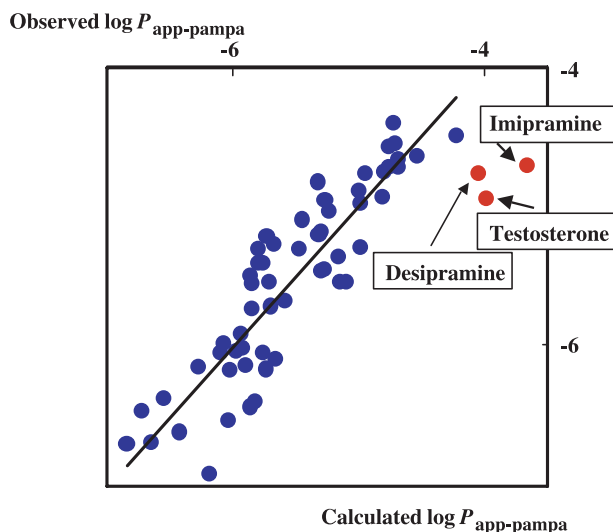


Figure 1. The relationship between observed and predicted artificial membrane permeability coefficients of 57 compounds. $\log P_{\text{app-pampa}}$ was predicted using Eq. 3. Three compounds: imipramine, testosterone, and desipramine (●) were excluded from Eq. 3.

mately constant regardless of the testosterone concentration, showing no effect of testosterone.

2.4. VolSurf analyses

The $\log P_{\text{app-pampa}}$ dataset of drugs was statistically analyzed by the PLS method using VolSurf.²⁰ Although no statistically significant equation was obtained for the drug dataset, Eq. 4 was formulated for PAMPA permeability of the compound set, including drugs and peptide-related compounds. The PLS coefficient of variables in Eq. 4 is given in Figure 3.

For all compounds including peptide-related compounds,

$$\log P_{\text{app-pampa}} = \text{VolSurf parameters} - 5.57.$$

$$\begin{aligned} \text{Component Number} &= 6 \quad n = 57, \quad SE_{\text{calcd}} = 0.39, \\ r^2 &= 0.69, \quad SE_{\text{pred}} = 0.56, \quad q^2 = 0.37, \end{aligned} \quad (4)$$

where SE_{calcd} and SE_{pred} are the standard deviations of error of calculations and predictions (leave-one-out), respectively.

Figure 3 indicates the larger the hydrophilic regions and hydrogen-bonding ability, the lower the membrane permeability. On the other hand, the larger the hydrophobic regions, the higher the permeability,

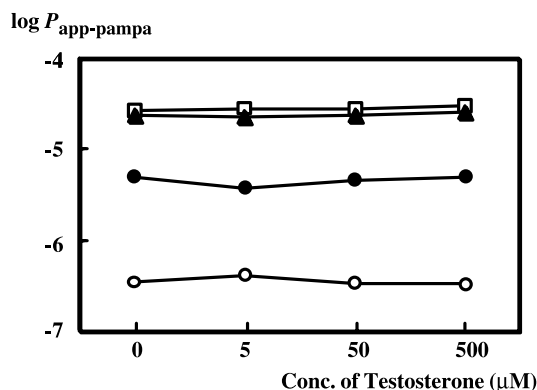


Figure 2. $\log P_{\text{app-pampa}}$ of pindolol (●), furosemide (○), propranolol (□), and verapamil (▲) in the presence of 5, 50, and 500 μM testosterone.

as expected. Factors such as local interaction energy minima, which represent the energy of the best three local minima of interaction energies between the water probe and the compound, decreased the membrane permeability of compounds, whereas a larger molecular packing increased the permeability. In general, integrity moments²⁰ and hydrophobic integrity moments, vectors pointing from the center of mass to the center of hydrophilic and hydrophobic regions, decreased and increased the permeability, respectively.

2.5. Relationship between Caco-2 cell and PAMPA permeability coefficients

In our previous report,¹⁶ we showed the relationship between $\log P_{\text{app-Caco-2}}$, where $P_{\text{app-Caco-2}}$ is the Caco-2 cell permeability coefficient at pH 7.3, and $\log P_{\text{app-pampa}}$ of peptide-related compounds. The $P_{\text{app-Caco-2}}$ values of commercial drugs at pH 7.4 were reported by Yazdani et al.²¹ as listed in Table 1. Figure 4 shows the relationship between the $\log P_{\text{app-Caco-2}}$ and $\log P_{\text{app-pampa}}$ values of drugs and peptide-related compounds. The peptide-related compounds were classified into three groups based on their bi-directional permeability coefficients across Caco-2 cells by our measurement: (1) passively transported compounds, (2) actively transported compounds, and (3) compounds excreted by efflux systems.¹⁵ In Figure 4, five compounds (indole-3-acetamide, indole-3-carboxylic acid, indole-3-acetic acid, indole-3-propionic acid, and salicylic acid) in group (2) were positioned above the correlation line, whereas three compounds [Ac-Trp-Val-NH₂, Ac-D-Trp-Val-NH₂, and *cyclo*(-Trp-Trp)] in group (3) were positioned below the line.

Table 2. Development of Eq. 3

Constant	$\log P_{\text{oct}}$	$ \text{p}K_{\text{a}} - \text{pH} $	SA_{HD}	SA_{HA}	r^2	s	$F_{x,y}$
-6.02	0.32				0.34	0.55	$F_{1,55} = 27.71$
-5.96	0.48	-0.24			0.52	0.47	$F_{2,54} = 29.16$
-5.41	0.43	-0.25	-1.23		0.68	0.38	$F_{3,53} = 38.33$
-4.93	0.42	-0.26	-1.01	-1.11	0.78	0.32	$F_{4,52} = 46.08$

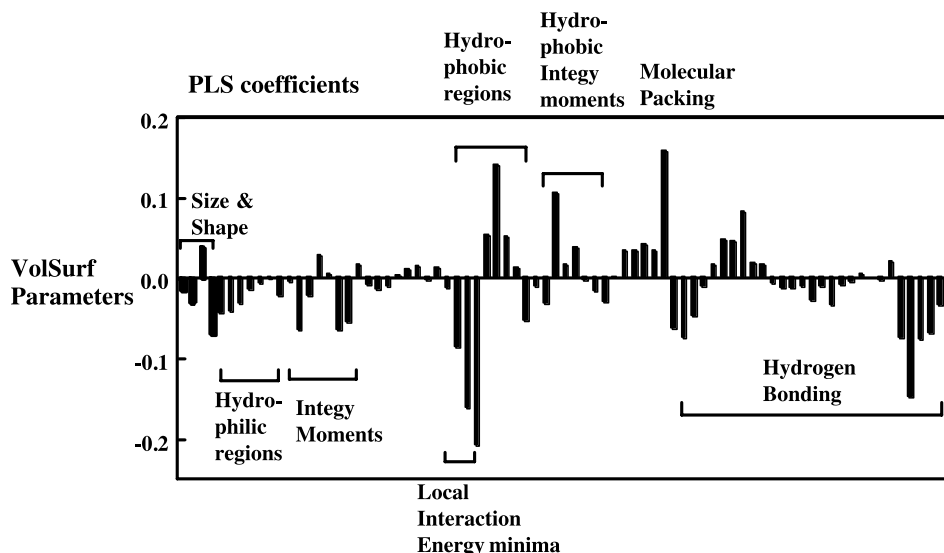


Figure 3. The PLS coefficient of variables in Eq. 4.

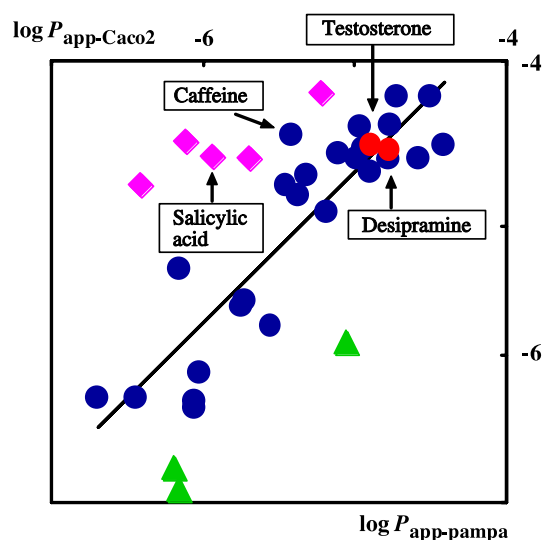


Figure 4. The relationship between the Caco-2 cell and artificial membrane permeability coefficients of compounds, including group (1) passively transported compounds (●), group (2) actively transported compounds (◆), and group (3) compounds excreted by efflux systems (▲). Testosterone and desipramine (●), which were excluded from Eq. 3, are included in passively transported compounds.

Only salicylic acid out of 21 drugs including testosterone and desipramine, for which $P_{\text{app-Caco-2}}$ values were reported, was considered to be actively transported (See Section 3). The other 20 drugs were classified into group (1) of passively transported compounds. The group number of each compound is shown in Table 1. For 27 compounds in total (20 drugs and 7 peptide-related compounds in group (1)), the correlation Eq. 5 was as follows:

$$\log P_{\text{app-Caco-2}} = 1.03(\pm 0.21) \log P_{\text{app-pampa}} + 0.39(\pm 1.10),$$

$$n = 27, s = 0.31, r^2 = 0.81, q^2 = 0.78. \quad (5)$$

In Eq. 5, the slope and intercept are very close to unity and zero, respectively, indicating that the Caco-2 cell permeability of these compounds completely corresponds to the artificial membrane permeability.

3. Discussion

3.1. Classical QSAR equations for the $\log P_{\text{app-pampa}}$

Several models for predicting absorption of drugs in humans have been developed using either experimental or computational approaches.^{10,22–29} A number of predictive models of drug Caco-2 cell permeability, which are known to show good correlations with oral absorption of drugs in humans,³⁰ have also been reported.^{31–36} Recently, permeation assay through artificial membranes such as PAMPA was developed in order to evaluate absorption across the membrane via the transcellular route.^{5–14,16} In our previous study,¹⁶ we indicated that the classical QSAR approach predicted the PAMPA permeability of peptide derivatives and related compounds. In addition, the relationship between Caco-2 cell permeability and artificial lipid-membrane permeability was determined. The compounds were sorted according to their absorption pathway in the plot of the Caco-2 cell and PAMPA permeability coefficients (passively transported compounds, actively transported compounds, and compounds excreted by efflux systems). In this study, we evaluated the PAMPA permeability of commercial drugs with more diverse structures and analyzed the permeability using descriptors, which represent physicochemical properties identical to those of peptides. PAMPA permeability increased with hydropho-

bicity and the higher ratio of neutral molecules, and decreased with the surface area occupied by hydrogen-bond acceptor/donor atoms. The $\log P_{\text{oct}}$ and $|\text{p}K_{\text{a}} - \text{pH}|$ terms explained 50% of the variation of PAMPA permeability coefficients (see Table 2).

There have been a few studies concerning the quantitative relationship between PAMPA or Caco-2 permeability and physicochemical parameters. The distribution coefficient, $\log D_{\text{oct}}$, and the polar surface area, PSA , have often been used for the prediction of intestinal absorption.^{25,26,37} It is possible to calculate the $\log D_{\text{oct}}$ value of ionizable compounds at a particular pH using Eq. 13 if the partition of ion-pair complexes is neglected. However, the ionized form of compounds usually moves to the hydrophobic phase making the ion-pair with counterions in the solution.³⁸ Thus, $\log D_{\text{oct}}$ values are dependent on buffer systems as well as pH of the solution. The result that the coefficients of the $|\text{p}K_{\text{a}} - \text{pH}|$ term are significantly smaller than those of the $\log P_{\text{oct}}$ term in Eqs. 1–3 suggests that a portion of the ion form of compounds permeates across the artificial membrane as ion-pair complexes. When the $\log D_{\text{oct}}$ value at pH 7.3 calculated according to Eq. 13 was therefore used for the classical QSAR analysis, a statistically worse equation than Eq. 3 was obtained ($n = 57$, $s = 0.37$, $r^2 = 0.71$, and $q^2 = 0.67$). The use of the combination of $\log P_{\text{oct}}$ and $|\text{p}K_{\text{a}} - \text{pH}|$ allows us to predict the artificial membrane permeability of ionizable compounds at any experimental pH.

As previously reported,¹⁶ only the hydrogen-accepting capability was significant in Eq. 2 for peptide-related compounds. On the other hand, in Eqs. 1 and 3 for drugs and a combined set of compounds, respectively, both the effects of hydrogen donor and acceptor atoms, SA_{HD} and SA_{HA} , were significant because the structure of drugs in this study was more diverse than peptide-related compounds. The coefficients of the SA_{HA} term in Eqs. 1 and 3 were more negative than those of the SA_{HD} term. We analyzed PAMPA permeability using PSA instead of SA_{HD} and SA_{HA} for comparison.

For diverse drugs

$$\begin{aligned} \log P_{\text{app-pampa}} = & 0.40(\pm 0.09) \log P_{\text{oct}} \\ & - 0.28(\pm 0.08) |\text{p}K_{\text{a}} - \text{pH}| \\ & - 0.99(\pm 0.32) PSA - 4.91(\pm 0.33), \\ n = 35, s = 0.27, r^2 = 0.83, q^2 = 0.79. \end{aligned} \quad (6)$$

For peptide-related compounds

$$\begin{aligned} \log P_{\text{app-pampa}} = & 0.48(\pm 0.20) \log P_{\text{oct}} \\ & - 0.29(\pm 0.16) |\text{p}K_{\text{a}} - \text{pH}| \\ & - 1.08(\pm 0.50) PSA - 5.04(\pm 0.59), \\ n = 22, s = 0.36, r^2 = 0.74, q^2 = 0.62. \end{aligned} \quad (7)$$

For all compounds

$$\begin{aligned} \log P_{\text{app-pampa}} = & 0.42(\pm 0.09) \log P_{\text{oct}} \\ & - 0.26(\pm 0.07) |\text{p}K_{\text{a}} - \text{pH}| \\ & - 1.05(\pm 0.27) PSA - 4.94(\pm 0.30), \\ n = 57, s = 0.32, r^2 = 0.78, q^2 = 0.75. \end{aligned} \quad (8)$$

Eqs. 6 and 8 have comparable s , r^2 , and q^2 with their counterparts, Eqs. 1 and 3, respectively, whereas the statistical quality of Eq. 7 for peptide-related compounds is much worse than that of Eq. 2. As described in Section 5.9, SA_{HD} and SA_{HA} correspond to the difference in the hydrogen-bonding capability of compounds for the artificial membrane and 1-octanol. Since the contribution of the hydrogen-donating and -accepting ability to permeation can differ, we adopted SA_{HD} and SA_{HA} rather than PSA as descriptors of the hydrogen-bonding capability.

3.2. Analysis with calculated physicochemical parameters

It was attempted to use the calculated $\log P_{\text{oct}}$ values by MacLogP software^{39,40} ($C \log P_{\text{oct}}$) and the calculated $\text{p}K_{\text{a}}$ values (calcd $\text{p}K_{\text{a}}$) by ACD software⁴¹ in place of the measured $\log P_{\text{oct}}$ and $\text{p}K_{\text{a}}$ values in Eq. 3. In fact, the correlation between the measured and calculated $\log P_{\text{oct}}$ values for the compound set in this study was high ($r^2 = 0.94$). Since the $|\text{calcd } \text{p}K_{\text{a}} - \text{pH}|$ values also correlated well with the $|\text{p}K_{\text{a}} - \text{pH}|$ values ($r^2 = 0.95$), Eq. 9 was obtained.

For all compounds

$$\begin{aligned} \log P_{\text{app-pampa}} = & 0.36(\pm 0.09) C \log P_{\text{oct}} \\ & - 0.24(\pm 0.09) |\text{calcd } \text{p}K_{\text{a}} - \text{pH}| \\ & - 1.24(\pm 0.53) SA_{\text{HA}} \\ & - 0.77(\pm 0.47) SA_{\text{HD}} - 4.86(\pm 0.33), \\ n = 57, s = 0.36, r^2 = 0.72, q^2 = 0.67. \end{aligned} \quad (9)$$

Although the statistical quality of Eq. 3, in which measured values were used, is better than Eq. 9, Eq. 9 is acceptable. Thus, the possibility for the in silico prediction of passive transport using calculated values was shown.

3.3. Compounds excluded from analyses for the $\log P_{\text{app-pampa}}$

Three compounds, imipramine, testosterone, and desipramine, were excluded from Eq. 3. The predicted $\log P_{\text{app-pampa}}$ values by Eq. 3 of imipramine, testosterone, and desipramine were -3.68 , -4.01 , and -4.08 , respectively, higher than the measured values, -4.71 , -4.95 , and -4.77 . Since the permeability coefficients of several compounds were not affected by the presence of testosterone, it is unlikely that properties of the artificial lecithin membrane were changed by testosterone. If the PAMPA permeability coefficient bilinearly depends on the $\log P_{\text{oct}}$ with the optimum $\log P_{\text{oct}}$ value,^{40,42} it is possible that $\log P_{\text{oct}}$ of imipramine, testosterone, and desipramine having considerably higher hydrophobicity ($\log P_{\text{oct}}$ values: imipramine, 4.44; tes-

tosterone, 3.32; desipramine, 4.54) is over the optimum, resulting in a lower permeability than expected. The bilinear analysis of the PAMPA permeability coefficients was performed including these three compounds and a significant equation was obtained.⁴³ However, the statistical quality of the equation was not very good ($n = 60$, $s = 0.35$, $r^2 = 0.75$, and $q^2 = 0.68$) and the permeability of the three compounds was not predicted well because of few hydrophobic compounds. Nielsen and Avdeef have reported that an unstirred water layer is the rate limiting barrier to transport through lipid membranes for lipophilic molecules.⁴⁴ This might be an alternative explanation for the lower permeability of imipramine, testosterone, and desipramine than that predicted in Eq. 3. Further studies are needed to clarify factors which influence the permeability of hydrophobic compounds.

3.4. VolSurf analyses

The PAMPA permeability for drugs was also analyzed using the VolSurf procedure. However, a significant result was obtained not for drugs, but the combined set of 57 compounds, including drugs and peptide-related compounds. A number of descriptors have been derived using four probes (water, DRY hydrophobic probe, carboxyl oxygen, and amide nitrogen) as described in Section 5. It is possible that these descriptors are too complicated to explain the variations in artificial membrane permeability, which is a simple physicochemical property. As a result, VolSurf may not be suitable for a set of compounds with diverse structures, such as drugs. Although we derived a significant VolSurf equation for the combined set of compounds (Eq. 4; Component Number = 6, $n = 57$, $SE_{\text{calc}} = 0.39$, $r^2 = 0.69$, $SE_{\text{pred}} = 0.56$, $q^2 = 0.37$), the statistical quality was much worse than that of the peptide set (compound 1–22) (Component Number = 4, $n = 22$, $SE_{\text{calc}} = 0.26$, $r^2 = 0.87$, $SE_{\text{pred}} = 0.43$, $r^2_{\text{pred}} = 0.65$, see Eq. 4 in Ref. 16). The tendency of the PLS coefficient of variables in Eq. 4 was similar to that of the peptide set.

3.5. Other PAMPA studies

The experimental artificial membrane permeability coefficients of drugs have been previously reported. Zhu et al. reported the artificial membrane permeability of 92 commercial drugs using a 96-well filtration plate (1% egg lecithin in *n*-dodecane).¹⁰ Sugano et al. measured the permeability coefficients of 80 structurally diverse compounds by a bio-mimetic artificial membrane permeation assay, in which the composition of the lipid membrane was modified to mimic the intestinal brush border membrane.⁸ Di et al. modified PAMPA for the prediction of blood–brain barrier penetration, using porcine polar brain lipid, and the assay was developed with 30 structurally diverse commercial drugs.¹³ Avdeef reported a number of permeability values, which were measured using a 10% w/v egg or soy lecithin in a dodecane PAMPA model at pH 7.4.⁴⁵ Since the artificial membrane permeability of a variety of drugs was measured using various lipids, solvents, and protocols in the above literatures, it was not easy

to compare the permeability obtained in this study with any other permeability. We used 10% lecithin in 1,9-decadiene for measurements. In the results, statistical equations predicting the measured PAMPA permeability of diverse compounds were obtained using the simple physicochemical properties such as $\log P$, pK_a , and surface area occupied by hydrogen donor and acceptor atoms. Since these properties do not depend on experimental conditions such as pH and buffer systems, our prediction model could provide a reliable permeability coefficient.

3.6. Relationship between Caco-2 cell and PAMPA permeability coefficients

We compared the measured PAMPA permeability with the Caco-2 permeability of 25 compounds in the literature²¹ (Fig. 4). In Figure 4, the permeability of drugs, except for salicylic acid and several peptide-related compounds, showed good correlation. Figure 4 also shows that salicylic acid is positioned above the line, indicating that salicylic acid is actively transported by monocarboxylic acid transporter, MCT1, in Caco-2 cells.⁴⁶ It is interesting that testosterone and desipramine, which were excluded from Eq. 3 for prediction of the PAMPA permeability, are included in the group (1): passively transported compounds.

It has previously been shown that acebutolol,⁴⁷ nadolol,⁴⁷ ranitidine,⁴⁸ and phenytoin⁴⁹ are excreted by P-gp although the Caco-2 permeability coefficients of these compounds correlated well with PAMPA permeability coefficients. This result suggests the importance of absorption by a transcellular mechanism for the compounds. Even if they are carried by transporter proteins, contribution by the route to total cell permeation could be small.

The passive paracellular pathway was not taken into account in this report because contribution by the route is usually small. It is often generalized that rapidly transported hydrophobic compounds are absorbed across the membrane by a transcellular route, whereas slowly transported hydrophilic compounds are absorbed through the tight junctions via a paracellular pathway.⁵⁰ However, the small surface area of the paracellular space and the gating function of tight junctions limit the paracellular absorption of hydrophilic drugs and peptides. It was reported that compounds with a molecular weight over 200 are absorbed only to a minor extent by the paracellular route.³³ The molecular weight of compounds is shown in Table 1. Of the compounds used in Figure 4, compounds with a molecular weight below 200 are indole derivatives 16, 17, and 19–22, caffeine and salicylic acid. Of these compounds, indole derivatives were previously determined to be either actively transported or passively transported through membranes based on the bi-directional permeability coefficients in Caco-2 cells. The Caco-2 permeability coefficient of caffeine was higher than that predicted from the PAMPA permeability coefficient in Figure 4, suggesting the possibility of contribution by the paracellular pathway. Salicylic acid also showed higher Caco-2 permeability than

predicted. However, as described above, since salicylic acid is actively transported by MCT1, it is unlikely that the paracellular pathway contributes to absorption of the compound.⁵¹

Recently Kerns et al.⁴⁹ discussed the relationship between PAMPA and Caco-2 permeability of drugs in a similar manner to our approach. However, no explanation based on physicochemical significance was identified for PAMPA permeability and no prediction model for PAMPA permeability was proposed in their paper. Our previous study¹⁶ was the first attempt to quantitatively analyze the PAMPA permeability of peptide-related compounds using simple physicochemical molecular properties on a theoretical basis and to show the predictive value of Caco-2 cell permeability using PAMPA. This study extended the previous study to a general theory for compounds with diverse structures.

4. Conclusions

In this study, we analyzed the permeability coefficients of diverse drugs and peptide-related compounds through artificial membranes using simple physicochemical properties in a classical QSAR procedure, and an *in silico* good prediction model for artificial membrane permeation was obtained. We also compared compounds transported by various absorption mechanisms and the compounds were sorted according to their absorption pathway. Although the passive transcellular route may be dominant, especially for drug transport across the intestinal epithelium,²¹ active transport mechanisms including the P-gp efflux system likely play a role in both Caco-2 cells and in humans, as in the case of several compounds, including salicylic acid. The contribution of each transport mechanism to the total permeability of compounds should be considered separately.

Therefore, the human intestinal absorption of a compound is predictable *in silico* according to the following steps.

- (1) Measurement or calculation of $\log P_{\text{oct}}$ and $\text{p}K_{\text{a}}$ of the compound. In the case of calculated values being used, it is important to use reliable values. Measurement of the $\log P_{\text{oct}}$ and $\text{p}K_{\text{a}}$ values of at least one or two compounds is recommended for comparison with the calculated values.
- (2) Construction of the 3D-structure and calculation of the surface area occupied by hydrogen donor and acceptor atoms, SA_{HD} and SA_{HA} .
- (3) Prediction of the permeability coefficient by the transcellular route using $\log P_{\text{oct}}$, $\text{p}K_{\text{a}}$, SA_{HD} , and SA_{HA} .
- (4) Prediction of the Caco-2 cell permeability coefficient of the compound from the permeability coefficient by the transcellular route if the compound is not a substrate of any transporters, including efflux systems.
- (5) Prediction of the human intestinal absorption from the Caco-2 cell permeability coefficient.
- (6) Evaluation of whether a compound is a substrate of a variety of transporters.

Although Willmann et al.⁵² proposed a human absorption model, only passive transport was postulated in their model. Recently, there have been several reports on the structure–activity relationships of substrates of the active transporters including efflux systems.^{53–57} If there were a reliable prediction model for these factors, *in silico* prediction for overall human absorption would be realistic using the above stepwise procedure.

5. Experimental

5.1. Materials

Thirty-eight commercial drugs were purchased from Nacalai Tesque (Kyoto, Japan), Kokusan Chemical Co. Ltd. (Tokyo, Japan), Wako Pure Chemical Industries (Osaka, Japan), Bachem AG (Bubendorf, Switzerland), Kanto Chemical (Tokyo, Japan), Sigma–Aldrich Japan (Tokyo, Japan) Tocris Cookson Ltd. (Bristol, UK) or BIOMOL Research Laboratories Inc. (PA, USA). Lecithin from egg yolk was purchased from Katayama Chemical Industries (Osaka, Japan). Hydrophobic filter plates (MultiScreen-IP, Clear Plates, 0.45 μm -diameter pore size), 96-well microplates, and 96-well UV-transparent microplates (COSTAR UV-plate) were obtained from Millipore (MA, USA), Asahi Techno Glass Corp. (Osaka, Japan), and Corning (MA, USA), respectively. All other reagents were of analytical grade and were purchased from Wako Pure Chemical Industries or Nacalai Tesque.

5.2. Permeability experiments with artificial membranes

Permeability experiments were carried out in 96-well microplates. A 96-well microplate (acceptor compartment) was completely filled with Tris–HCl buffer (pH 7.3) containing 5% DMSO. A hydrophobic filter plate (donor compartment) was fixed on the buffer-filled plate. The filter surface was impregnated with 5 μL of 10% (v/v) lecithin solution in 1,9-decadiene. A 200–500 μM compound solution in the same buffer containing 5% DMSO was prepared depending upon the compound solubility. A 200 μL sample of the compound solution was added to the filter plate and incubated at 25 °C for 2, 5 or 24 h. The filter plate was carefully removed and 200 μL of the solution in the acceptor compartment was placed on a UV-transparent microplate. The concentration of the solution in the UV-plate was then determined by UV spectroscopy, using the microtiter plate reader (Molecular Devices, spectra MAX 250 or FLUOstar OPTIMA) at 260 or 280 nm. A reference solution defining equilibrium conditions was prepared at the same concentration as the sample solution with no membrane barrier. The filter surface was wetted with 5 μL of a 60% (v/v) methanol/buffer solution for the reference. The permeability coefficient through the artificial membrane, $P_{\text{app-pampa}}$, was calculated using Eq. 10.⁶

$$P_{\text{app-pampa}} = -V_D V_R / [(V_D + V_R) A t] \cdot \ln(1 - OD_{\text{sam}} / OD_{\text{ref}}). \quad (10)$$

In this equation, V_D (cm^3) is the donor volume (0.2 cm^3), V_R (cm^3) is the volume of the acceptor compartment (0.38 cm^3), A (cm^2) is the accessible filter area (0.283 cm^2), and t (s) is the incubation time. OD_{sam} and OD_{ref} are the optical densities (OD) at 260 or 280 nm of the sample and reference solutions in the acceptor compartment, respectively.

5.3. Effect of testosterone on permeability coefficients

The permeability coefficients of 500 μM pindolol, furosemide, propranolol, and verapamil were determined in the presence of 5, 50, and 500 μM testosterone. The $P_{\text{app-pampa}}$ of the four compounds was calculated using Eq. 10 and OD_{sam} values after subtracting the optical density of the testosterone solutions in the acceptor compartment from the permeability measurement of 5, 50, and 500 μM testosterone only.

5.4. The partition coefficient P_{oct} and the dissociation constant K_a

For the $\log P_{\text{oct}}$ value, the measured values were available from the database of MacLogP software, version 4.0.^{39,40} The calculated $\log P_{\text{oct}}$ values, $\text{Clog } P_{\text{oct}}$, were also obtained using the MacLogP software. Their $\text{p}K_a$ values were obtained from CQSAR Database.⁴³ The calculated $\text{p}K_a$ values, $\text{calcd } \text{p}K_a$, were derived using ACD software.⁴¹ The absolute value of the difference between the $\text{p}K_a$ value of the compound and the experimental pH (7.3), $|\text{p}K_a - \text{pH}|$, was used for QSAR analyses as a descriptor. The $\log P_{\text{oct}}$, $\text{Clog } P_{\text{oct}}$, $|\text{p}K_a - \text{pH}|$, and $|\text{calcd } \text{p}K_a - \text{pH}|$ values are listed in Table 1.

5.5. Molecular modeling

All computations were performed using the molecular modeling software package SYBYL, version 6.8.⁵⁸ To select the initial conformation of compounds, we started from the coordinates of the X-ray crystallographic data for each compound obtained from the Cambridge Structure Database,⁵⁹ if available. The X-ray structure of each compound was geometry optimized by the Tripos force field to give a relatively stable conformer. The structures of practolol, metoprolol, and nadolol were constructed by modifying the energy-optimized structure of acebutolol. Structures of oxprenolol and hydrocortisone were constructed from the structures of alprenolol and corticosterone, respectively. The coordinates of the modified parts of these structures were calculated using the SYBYL standard values for bond lengths and angles. A systematic search in SYBYL was applied to all rotatable bonds. The low-energy conformer of each compound obtained by a systematic search was then geometry optimized by the Tripos force field. All compounds were modeled in their neutral form.

5.6. Surface area calculations

MOLPROP in SYBYL was used to calculate the surface area occupied by the hydrogen-bond acceptor and donor atoms of each modeled conformer (SA_{HA} and SA_{HD} [$\text{\AA}^2 \times 1/100$], respectively). The hydrogen-bond acceptor atoms were defined as nitrogen and oxygen atoms while the hydrogen-bond donor atoms were defined as hydrogen atoms attached to these heteroatoms. We also calculated the number of hydrogen-bond acceptor and donor atoms, the polar and non-polar parts of the surface area (PSA and $NPSA$ [$\text{\AA}^2 \times 1/100$], respectively), and the fraction of each surface area ($\%SA_{\text{HD}}$, $\%SA_{\text{HA}}$, $\%PSA$, and $\%NPSA$). However, the introduction of these parameters, except PSA , did not improve the statistical quality of classical QSAR equations.

5.7. Classical QSAR

PAMPA permeability, $\log P_{\text{app-pampa}}$, was quantitatively analyzed using the classical QSAR technique. Classical QSAR analyses were performed with QREG, version 2.05.⁶⁰ The bilinear analysis was carried out with CQSAR software.⁴³

5.8. VolSurf

To describe the 3D molecular field of the compound, the GRID force field (GRID software, version 18⁶¹) was used. Four probes (water, DRY, carboxyl oxygen, and amide nitrogen) were used to characterize the interaction sites around target molecules. “DRY” is a hydrophobic probe defined in VolSurf. Three-dimensional molecular field maps were transformed into 88 descriptors by VolSurf, version 3.07, which was developed as a 3D-QSAR procedure for predicting the ADME properties of a molecule.²⁰ These descriptors were molecular volume (V); surface (S); molecular weight (MW); critical packing (CR), which predicts molecular packing; size of the hydrophilic (W) and hydrophobic (D) regions; hydrogen-bonding properties (HB); integrity moments and hydrophobic integrity moments which are vectors pointing from the center of the mass to the center of hydrophilic and hydrophobic regions, respectively; local interaction energy minima which represent the energy of the best three local minima of interaction energies between the water probe and the compound, and so on. A more detailed representation of VolSurf descriptors has been presented by Cruciani et al.⁶²

The correlation of the PAMPA permeability coefficient with the data matrix was analyzed by the partial least squares (PLS) method.⁶³ The analysis results were expressed as correlation equations with the optimum number of latent variable or component terms, each of which was a linear combination of original independent lattice variables. We initially selected the number of components in the set as the number of cross-validations (the leave-one-out method) and then performed the analysis using the optimum number of latent variables deduced from the cross-validation tests without actual cross-validation. To derive the best equation, 79 out of 88 VolSurf descriptors were selected by the FFD variable selection method in VolSurf according to the pre-

dictive ability of the model equation with the presence or absence of each descriptor.

5.9. Theoretical basis or theoretical calculations

5.9.1. Hydrophobicity parameters. Eqs. 11 and 12 represent the relationship between $\log D_{\text{oct}}$, the distribution coefficient of compounds at a particular pH, and $\log P_{\text{oct}}$, defined as the partition coefficient of neutral forms, for acids and bases, respectively, if the partition of ion-pair complexes can be neglected.⁶⁴

For acids: $\log D_{\text{oct}} = \log P_{\text{oct}} - \text{pH} - \log(K_{\text{a}} + [\text{H}^+])$,
(11)

For bases: $\log D_{\text{oct}} = \log P_{\text{oct}} - \text{p}K_{\text{a}} - \log(K_{\text{a}} + [\text{H}^+])$.
(12)

$[\text{H}^+]$ is the hydrogen ion concentration of the aqueous phase. According to Eqs. 11 and 12, $\log D_{\text{oct}} = \log P_{\text{oct}}$ for acids when $\text{pH} \ll \text{p}K_{\text{a}}$ and for bases when $\text{pH} \gg \text{p}K_{\text{a}}$ (K_{a} is the acid dissociation constant of the conjugate acids). For acids, when $\text{pH} \gg \text{p}K_{\text{a}}$, $[\log D_{\text{oct}} = \log P_{\text{oct}} + \text{p}K_{\text{a}} - \text{pH}]$, whereas for bases, when $\text{pH} \ll \text{p}K_{\text{a}}$, $[\log D_{\text{oct}} = \log P_{\text{oct}} - \text{p}K_{\text{a}} + \text{pH}]$. These equations are unified to one Eq. 13.

$$\log D_{\text{oct}} = \log P_{\text{oct}} - |\text{p}K_{\text{a}} - \text{pH}|, \quad (13)$$

where $|\text{p}K_{\text{a}} - \text{pH}|$ is the absolute value of the difference between the $\text{p}K_{\text{a}}$ value of the compound and the experimental pH, representing the ratio of the ionized molecules to the neutral molecules. In this situation, the coefficients of $\log P_{\text{oct}}$ and $|\text{p}K_{\text{a}} - \text{pH}|$ terms should have same values in the following analyses, and these two terms can be replaced with $\log D_{\text{oct}}$. Thus, we used $\log P_{\text{oct}}$ and $|\text{p}K_{\text{a}} - \text{pH}|$ as the hydrophobicity parameter of compounds in order to examine whether the partition of ion-pair complexes can be neglected.

5.10. Hydrogen-bonding capability

Fujita et al. generalized the following equation for partition coefficients in different solvents from 1-octanol and water system.⁶⁵

$$\log P_{\text{solv}} = \log P_{\text{oct}} + \Delta \log f(\text{HB}) + \text{const.}, \quad (14)$$

$$\Delta \log f(\text{HB}) = \log[f(\text{HB})_{\text{solv}}/f(\text{HB})_{\text{oct}}]. \quad (15)$$

The $f(\text{HB})$ term is formulated with solvent molarity and the association equilibrium constant for compounds and a solvent. Thus, the $\Delta \log f(\text{HB})$ term relates to the difference in the hydrogen-bonding capability of compounds for a solvent and 1-octanol. Since both octanol and the artificial membrane (lecithin solution in 1,9-decadiene) have an amphiprotic character, it is not easy to theoretically determine whether either hydrogen-accepting or -donating ability, or both, gave an extra effect on the artificial membrane permeation when $\log P_{\text{oct}}$ was used as a reference to estimate hydrophobicity. Thus, both

the surface area occupied by the hydrogen-bond acceptor and donor atoms of each modeled conformer (SA_{HA} and SA_{HD}) were used as hydrogen-bond descriptors.

Acknowledgments

We are grateful to Emeritus Professor Toshio Fujita (Kyoto University) for his helpful advice and comments on QSAR. This work was supported in part by a Grant-in-Aid for Scientific Research (16510158) from the Ministry of Education, Culture, Sports, Science and Technology of Japan.

References and notes

- Lin, J.; Sahakian, D. C.; de Moraes, S. M. F.; Xu, J. J.; Polzer, R. J.; Winter, S. M. *Curr. Top. Med. Chem.* **2003**, *3*, 1125.
- Liang, R.; Fei, Y.-J.; Prasad, P. D.; Rammamoorthy, S.; Han, H.; Yang-Feng, T. L.; Hediger, M. A.; Ganapathy, V.; Leibach, F. H. *J. Biol. Chem.* **1995**, *270*, 6456.
- Tamai, I.; Takanaga, H.; Maeda, H.; Sai, Y.; Ogihara, T.; Higashida, H.; Tsuji, A. *Biochem. Biophys. Res. Commun.* **1995**, *214*, 482.
- Ueda, K.; Cornwell, M. M.; Gottesman, M. M.; Pastan, I.; Roninson, I. B.; Ling, V.; Riordan, J. R. *Biochem. Biophys. Res. Commun.* **1986**, *141*, 956.
- Kansy, M.; Senner, F.; Gubernator, K. *J. Med. Chem.* **1998**, *41*, 1007.
- Wohnsland, F.; Faller, B. *J. Med. Chem.* **2001**, *44*, 923.
- Sugano, K.; Hamada, H.; Machida, M.; Ushio, H. *J. Biomol. Screen.* **2001**, *6*, 189.
- Sugano, K.; Takata, N.; Machida, M.; Saitoh, K.; Terada, K. *Int. J. Pharm.* **2002**, *241*, 241.
- Sugano, K.; Nabuchi, Y.; Machida, M.; Aso, Y. *Int. J. Pharm.* **2003**, *257*, 245.
- Zhu, C.; Jiang, L.; Chen, T. M.; Hwang, K. K. A. *Eur. J. Med. Chem.* **2002**, *37*, 399.
- Veber, D. F.; Johnson, S. R.; Cheng, H. Y.; Smith, B. R.; Ward, K. W.; Kopple, K. D. *J. Med. Chem.* **2002**, *45*, 2615.
- Kerns, E. H. *J. Pharm. Sci.* **2001**, *90*, 1838.
- Di, L.; Kerns, E. H.; Fan, K.; McConnel, O. J.; Carter, G. T. *Eur. J. Med. Chem.* **2003**, *38*, 223.
- Obata, K.; Sugano, K.; Machida, M.; Aso, Y. *Drug Dev. Ind. Pharm.* **2004**, *30*, 181.
- Ano, R.; Kimura, Y.; Urakami, M.; Shima, M.; Matsuno, R.; Ueno, T.; Akamatsu, M. *Bioorg. Med. Chem.* **2004**, *12*, 249.
- Ano, R.; Kimura, Y.; Shima, M.; Matsuno, R.; Ueno, T.; Akamatsu, M. *Bioorg. Med. Chem.* **2004**, *12*, 257.
- Hansch, C.; Fujita, T. *J. Am. Chem. Soc.* **1964**, *86*, 1616.
- Sunamoto, J.; Hamada, T.; Murase, H. *Bull. Chem. Soc. Jpn.* **1980**, *53*, 2773.
- Miyoshi, H.; Maeda, H.; Tokutake, N.; Fujita, T. *Bull. Chem. Soc. Jpn.* **1987**, *60*, 4357.
- Cruciani, G.; Pastor, M.; Guba, W. *Eur. J. Pharm. Sci.* **2000**, *11*, S29.
- Yazdani, M.; Glynn, S. L.; Wright, J. L.; Hawa, A. *Pharm. Res.* **1998**, *15*, 1490.
- William, S.; Schmitt, W.; Keldenich, J.; Lippert, J.; Jennifer, B. *J. Med. Chem.* **2004**, *47*, 4022.
- Stenberg, P.; Norinder, U.; Luthman, K.; Artursson, P. *J. Med. Chem.* **2001**, *44*, 1927.

24. Klopman, G.; Stefan, L. R.; Saiakhov, R. *Eur. J. Pharm. Sci.* **2002**, *17*, 253.
25. Parrott, N.; Lavé, T. *Eur. J. Pharm. Sci.* **2002**, *17*, 56.
26. Palm, K.; Luthman, K.; Ungell, A.-L.; Strandlund, G.; Artursson, P. *J. Pharm. Sci.* **1996**, *85*, 32.
27. Yoshida, F.; Topliss, J. G. *J. Med. Chem.* **2002**, *43*, 2575.
28. Kobayshi, M.; Sada, N.; Sugawara, M.; Iseki, K.; Miyazaki, K. *Int. J. Pharm.* **2001**, *221*, 87.
29. Wessel, M. D.; Jurs, P. C.; Tolani, J. W.; Muskal, S. M. *J. Chem. Inf. Comput. Sci.* **1998**, *38*, 726.
30. Artursson, P.; Karlsson, J. *Biochem. Biophys. Res. Commun.* **1991**, *175*, 880.
31. Hou, T. J.; Zhang, W.; Xia, K.; Qiao, X. B.; Xu, X. J. *J. Chem. Inf. Comput. Sci.* **2004**, *44*, 1585.
32. Ren, S.; Lien, E. *J. Prog. Drug Res.* **2000**, *54*, 1.
33. Van de Waterbeemd, H.; Cameisch, G.; Folkers, G.; Raevsky, O. A. *Quant. Struct.-Act. Relat.* **1996**, *15*, 480.
34. Kulkarni, A.; Han, Y.; Hopfinger, A. J. *J. Chem. Inf. Comput. Sci.* **2002**, *42*, 331.
35. Camenisch, G.; Alsenz, J.; van de Waterbeemd, H.; Folkers, G. *Eur. J. Pharm. Sci.* **1998**, *6*, 313.
36. Goodwin, J. T.; Mao, B.; Vidmar, T. J.; Conrani, R. A.; Burton, P. S. *J. Peptide Res.* **1999**, *53*, 355.
37. Bergström, C. A. S.; Strafford, M.; Lazorova, L.; Avdeef, A.; Luthman, K.; Arturson, P. *J. Med. Chem.* **2003**, *46*, 558.
38. Akamatsu, M.; Yoshida, Y.; Nakamura, H.; Asao, M.; Iwamura, H.; Fujita, T. *Quant. Struct.-Act. Relat.* **1989**, *8*, 195.
39. MacLogP 4.0; Biobyte Corp.: Claremont, CA, USA.
40. Hansch, C.; Leo, A. *Exploring QSAR*; American Chemical Society: Washington, DC, 1995.
41. ACD/pKa DB, version 8.0; Advanced Chemistry Development, Inc., Toronto, Ont., Canada.
42. Kubinyi, H. *Arzneim.-Forsch.* **1979**, *29*, 1067.
43. CQSAR; Biobyte Corp.: Claremont, CA, USA.
44. Nielsen, P. E.; Avdeef, A. *Pharm. Sci.* **2004**, *22*, 33.
45. Avdeef, A. *Absorption and Drug Development*; Wiley-Interscience: New Jersey, 2003.
46. Kido, Y.; Tamai, I.; Okamoto, M.; Suzuki, F.; Tsuji, A. *Pharm. Res.* **2000**, *17*, 55.
47. Terao, T.; Hisanaga, E.; Sai, Y.; Tamai, I.; Tsuji, A. *J. Pharm. Pharmacol.* **1996**, *48*, 1083.
48. Lee, K.; Kim, C. N. G.; Brouwer, L. R.; Thakker, D. R. *J. Pharm. Exp. Ther.* **2002**, *303*, 574.
49. Kerns, E. H.; Di, L.; Petusky, S.; Farris, M.; Ley, R.; Jupp, P. *J. Pharm. Sci.* **2004**, *93*, 1440.
50. Cereijido, M.; Ruiz, O.; Gonzalez-mariscal, L.; Contreras, R. G.; Balda, M. S.; Garcia-Villegas, M. R. In *Biological Barriers to Protein Delivery*; Audus, K. L., Raub, T., Eds.; Plenum Press: New York, USA, 1993, pp 3–21.
51. Pade, V.; Stavchansky, S. *Pharm. Res.* **1997**, *14*, 1210.
52. Willmann, S.; Schmitt, W.; Keldenich, J.; Lippert, J.; Dressman, J. B. *J. Med. Chem.* **2004**, *16*, 4022.
53. Potschka, H.; Löscher, W. *Epilepsia* **2001**, *42*, 1231.
54. Wiese, M.; Pajeva, I. K. *Curr. Med. Chem.* **2001**, *8*, 685.
55. Kim, K. H. *Bioorg. Med. Chem.* **2001**, *9*, 1517.
56. Ekins, S.; Kim, R. B.; Leake, B. F.; Dantzig, A. H.; Schuetz, E. G.; Lan, L.-B.; Yasuda, K.; Shepard, R. L.; Winter, M. A.; Schuetz, J. D.; Winkel, J. H.; Wrighton, S. A. *Mol. Pharmacol.* **2002**, *61*, 964.
57. Wang, R. B.; Kuo, C. L.; Lien, L. L.; Lien, E. J. *J. Clin. Pharm. Ther.* **2003**, *28*, 203.
58. SYBYL Molecular Modeling Software; Tripos Associates, Inc.: St. Louis, MO, USA.
59. The Cambridge Structural Database; CCSD: Cambridge, UK.
60. Asao, M.; Shimizu, R.; Nakao, K.; Nishioka, T.; Fujita, T. QREG 2.05; Japan Chemistry Program Exchange: Ibaraki, Japan.
61. Goodford, P. J. *J. Med. Chem.* **1985**, *28*, 849.
62. Cruciani, G.; Crivori, P.; Carrupt, P.-A.; Testa, B. *J. Mol. Struct. (Theochem)* **2000**, *503*, 17.
63. Wold, S.; Ruhe, A.; Wold, H.; Dunn, W. J., III *SIAM J. Sci. Stat. Comput.* **1984**, *5*, 735.
64. Terada, H.; Kitagawa, K.; Yoshikawa, Y.; Kametani, F. *Chem. Pharm. Bull.* **1981**, *29*, 7.
65. Fujita, T.; Nishioka, T.; Nakajima, M. *J. Med. Chem.* **1977**, *20*, 1071.